

## STABILIZATION OF PENDULUM IN VARIOUS INCLINATIONS USING OPEN-LOOP CONTROL

Maciej CIĘŻKOWSKI\*

\*phD student, Department of Automatics and Robotics, Faculty of Mechanical Engineering,  
 Białystok University of Technology, ul. Wiejska 45 C, 15-351 Białystok

[mciezkowski@gmail.com](mailto:mciezkowski@gmail.com)

**Summary:** The paper presents the stabilization method of physical pendulum in various inclinations. The theory of the motion in a rapidly oscillating field has been applied to explain the phenomenon of stabilization and to set conditions for the stability of the pendulum. The paper shows results of computer simulations which confirm that the position control of the pendulum in the open-loop is possible.

### 1. INTRODUCTION

The inverted pendulum, which is physical pendulum, whose center of mass lies above the point of suspension is very popular pendulum tested in automatics. It is an example of a nonlinear system characterized by high instability. Due to its properties it is a good object for testing different control algorithms. Beside the fact the system is interesting from a theoretical point of view, it has many practical applications: stabilization of a walking robot, rocket flight control (Astrom and Murray, 2008), or recently popular two-wheeled vehicle - "Segway".

Most of studies on inverted pendulum concern a closed-loop control. There is also a way to stabilize the pendulum in the open-loop control, where the pendulum suspension point performs fast oscillations in the vertical direction (Kapica, 1951; Siemieniako and Ciężkowski, 2011). Oscillations of the suspension point in the horizontal direction gives an interesting result, namely the possibility of stabilizing the pendulum between a horizontal and hanging position (Landau and Lifshitz, 2007; Siemieniako and Ciężkowski, 2011). It turns out that it is possible to generalize the problem and demonstrate the possibility of stabilization of the pendulum in various positions with oscillating point of suspension at the appropriate angle, which will be the subject of this paper.

### 2. MODEL OF PENDULUM

The perfectly rigid rod has been taken as the model of the pendulum, with mass  $m$  and length  $l$ . One end of the pendulum is the point of suspension. The system is placed in a gravitational field with a value of acceleration  $g$ . Fig. 1 shows the physical model of the pendulum. The system has been described by the Lagrange formalism.

The position of the suspension point of the pendulum describes vector:

$$\mathbf{r}_b = (A \cos(\Omega t) \sin(\beta), A \cos(\Omega t) \cos(\beta)) \quad (1)$$

where:  $A$  – amplitude vibrations of the suspension point,

$\Omega$  – the frequency of the vibrations,  $\beta$  – angle, the direction of vibration of the suspension point.

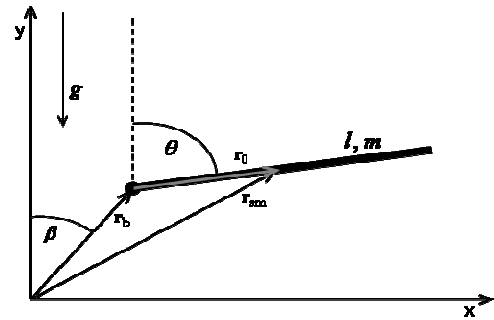


Fig. 1. Physical model of pendulum

The position of the mass center of the pendulum relative to the suspension is:

$$\mathbf{r}_0 = \frac{1}{2} l (\sin \theta, \cos \theta) \quad (2)$$

where:  $\theta$  – the pendulum angle with respect to the y-axis.

Position of the mass center relative to the origin of the coordinate system is:

$$\mathbf{r}_{sm} = \mathbf{r}_b + \mathbf{r}_0 = \left( \frac{1}{2} l \sin \theta + A \cos(\Omega t) \sin(\beta), \frac{1}{2} l \cos \theta + A \cos(\Omega t) \cos(\beta) \right) \quad (3)$$

The kinetic energy is the sum of the translational kinetic energy of the mass center and the rotational kinetic energy of the pendulum relative to the mass center:

$$T = \frac{1}{2} m \dot{\mathbf{r}}_{sm}^2 + \frac{1}{2} \frac{1}{12} m l^2 \dot{\theta}^2 = \frac{1}{6} m (3A^2 \Omega^2 \sin^2(\Omega t) + \dot{\theta} l (\dot{\theta} l - 3A \Omega \sin(\beta - \theta) \sin(\Omega t))) \quad (4)$$

The potential energy of system is:

$$V = gm (A \cos(\beta) \cos(t \Omega) + \frac{1}{2} l \cos(\theta)) \quad (5)$$

The Lagrangian has the form:

$$L = T - V \quad (6)$$

Substituting (4) and (5) into equation (6) then solving the Euler-Lagrange equation we get:

$$\frac{d}{dt} \frac{\partial L}{\partial \dot{\theta}} = \frac{\partial L}{\partial \theta} \Rightarrow \ddot{\theta} = \frac{3(A\Omega^2 \sin(\beta - \theta) \cos(t\Omega) + g \sin(\theta))}{2l} \quad (7)$$

The obtained equation is an equation of motion of the pendulum.

### 3. MOTION ANALYSIS OF PENDULUM AS THE MOTION IN A RAPIDLY OSCILLATING FIELD

Oscillating change of the suspension point's position realizes the pendulum's control. It is assumed that the frequency of these oscillations is large compared with the oscillation frequency of the system if the movement takes place only under the influence of the gravity. It is also assumed that the changes of the pendulum's position, caused by these vibrations, are small. Such an object can be regarded as an object moving in a rapidly oscillating field.

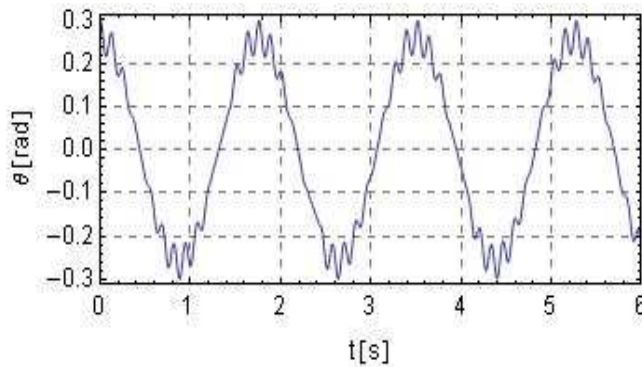


Fig. 2. Numerical simulation result

Fig. 2 (Siemieniako and Ciężkowski, 2011) shows the simulation results of the pendulum angle's time-variation. This is a solution of the equation (7) for values:

$$l = 1m, g = 9.81 \frac{m}{s^2}, A = 0.1m, \Omega = 50 \frac{rad}{s}, \beta = 0rad,$$

$$\theta(0) = 0.3rad, \dot{\theta}(0) = 0 \frac{rad}{s}$$

It can be noted that the swing of the pendulum is composed of vibrations of high amplitude and low frequency (hereinafter referred to as  $\Phi(t)$ ) and small oscillations of high frequency ( $\xi(t)$ ). The presence of small oscillations appears to be consistent with the assumptions, if the movement takes place in a constant gravity field and rapidly oscillating field which enforces the oscillations of the suspension point. If the motion is a combination of two oscillations, the position of the pendulum can be written as:

$$\theta(t) = \Phi(t) + \xi(t) \quad (8)$$

where  $\Phi(t)$  describes the "smooth" movement of the pendulum, averaged due to the rapid oscillations.

Substituting (8) to (7) and expanding the result in the first-order Taylor series because of the  $\xi$  (small oscillations) the following is obtained:

$$\ddot{\Phi} + \ddot{\xi} = -\frac{3A\xi\Omega^2 \cos(\beta - \Phi) \cos(t\Omega)}{2l} + \frac{3A\Omega^2 \sin(\beta - \Phi) \cos(t\Omega)}{2l} + \frac{3g\xi \cos(\Phi)}{2l} + \frac{3g \sin(\Phi)}{2l} \quad (9)$$

Acceleration of the suspension point is proportional to  $\Omega^2$  and changes quickly. It can be concluded that the  $\xi$  will meet the same relationship. Only the second term of the equation (9) satisfies these conditions (first term is proportional to  $\xi$ , so it is small). So you can write:

$$\ddot{\xi} = \frac{3A\Omega^2 \sin(\beta - \Phi) \cos(t\Omega)}{2l} \quad (10)$$

The value of  $\ddot{\Phi}$  is equal to the other terms of the equation (9):

$$\ddot{\Phi} = -\frac{3A\xi\Omega^2 \cos(\beta - \Phi) \cos(t\Omega)}{2l} + \frac{3g\xi \cos(\Phi)}{2l} + \frac{3g \sin(\Phi)}{2l} \quad (11)$$

Double-integrating expression (10) under the assumption that  $\Phi$  changes so slowly that we can consider them as constants, we get:

$$\xi = -\frac{3A \cos(t\Omega) \sin(\beta - \Phi)}{2l} \quad (12)$$

Substituting equation (12) to (11) and averaging the result due to the rapid oscillations ( $\overline{\cos(t\Omega)} = 0, \overline{\cos(t\Omega)^2} = 1/2$ ) we obtain the equation:

$$\ddot{\Phi} = \frac{9A^2\Omega^2 \sin(2(\beta - \Phi))}{16l^2} + \frac{3g \sin(\Phi)}{2l} \quad (13)$$

To show why the pendulum is stable it has to be determined what the effective potential energy of the system is:

$$\frac{1}{3} ml^2 \ddot{\Phi} = -\frac{dU_{ef}}{d\Phi} \Rightarrow U_{ef} = -\frac{1}{3} ml^2 \int \ddot{\Phi} d\Phi \Rightarrow \quad (14)$$

$$U_{ef} = \frac{1}{2} glm \cos(\Phi) - \frac{3}{32} A^2 m \Omega^2 \cos(2(\beta - \Phi))$$

Fig. 3 illustrates the graph of function (14) for different values of angle  $\beta$ , for fixed  $g, m, l, A, \Omega$  equal to:  $g = 9,81 m/s^2, m = 0,8 kg, l = 1m, A = 0,1 m, \Omega = 70 rad/s$ .

The meaning of the line is as follows:

- solid line:  $\beta = 0$ ;
- dotted line:  $\beta = \pi/4$ ;
- "dot-dash" line:  $\beta = \pi/2$ ;
- dashed line:  $\beta = 3/4\pi$ .

As shown in the Fig. 3 each plot has a minimum of the potential (and thus satisfies the condition of the stability), which for fixed parameters  $g, m, l, A, \Omega$  is dependent on the

angle  $\beta$ . This relationship has been found, what will be the subject of the next chapter.

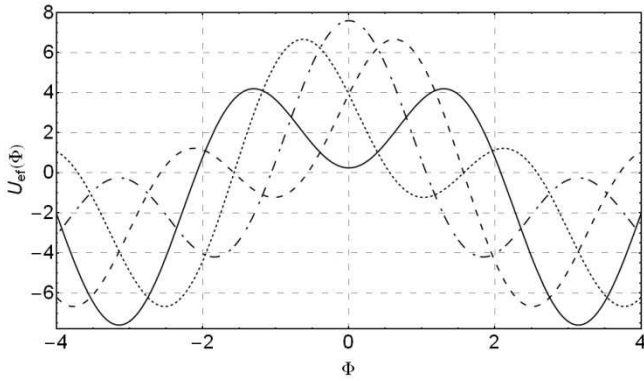


Fig. 3. Effective potential of the pendulum for various values of  $\beta$

#### 4. STABILITY CONDITIONS

Conditions for a minimum potential at a given point are: the first derivative  $U_{ef}$  is zero and the second derivative of the effective potential energy is positive at this point.

The first derivative of equation (14) is:

$$\frac{\partial U_{ef}}{\partial \Phi} = -\frac{3}{16} A^2 m \Omega^2 \sin(2(\beta - \Phi)) - \frac{1}{2} g l m \sin(\Phi) \quad (15)$$

Denoting:

$$\lambda = \frac{3A^2 \Omega^2}{4gl} \quad (16)$$

the extreme condition can be written as:

$$\frac{\partial U_{ef}}{\partial \Phi} = 0 \Leftrightarrow \sin(\Phi) + \frac{1}{2} \lambda \sin(2(\beta - \Phi)) = 0 \quad (17)$$

and can be solved for variable  $\beta$ . Solution of equation (17) gives the result:

$$\beta = \beta_{ext} = \frac{1}{2} (2\Phi - \arcsin(\frac{2 \sin(\Phi)}{\lambda})) \quad (18)$$

The second derivative of the potential for  $\beta = \beta_{ext}$  is:

$$\frac{\partial^2 U_{ef}}{\partial \Phi^2} |_{\beta=\beta_{ext}} = \frac{1}{8} (3A^2 m \Omega^2 \sqrt{1 - \frac{4 \sin^2(\Phi)}{\lambda^2}} - 4gl m \cos(\Phi)) \quad (19)$$

Requesting it to be greater than zero, conditions for the existence of a minimum of effective potential are:

I)

$$\lambda > \sqrt{4 \sin^2(\Phi) + \cos^2(\Phi)} \quad \text{for } \Phi \in (0, \frac{\pi}{2}) \quad (20)$$

II)

$$\lambda > 2 \quad \text{for } \Phi = \frac{\pi}{2} \quad (21)$$

III)

$$\lambda \geq 2 \sin(\Phi) \quad \text{for } \Phi \in (\frac{\pi}{2}, \pi) \quad (22)$$

These conditions can be compared with the results for vertical and horizontal oscillations contained in the publication Siemięniako and Ciężkowski (2011): when the angle  $\Phi = 0$  (the case of vertical oscillations) then according to (20) the stability condition is:  $\lambda > 1$ .

When  $\Phi = \arccos(-1/\lambda)$  (the case of horizontal oscillations) then according to (22) the stability condition is:  $\lambda > 1$ .

In both cases, the stability conditions are the same as in the publication of the above mentioned authors.

#### 4.1. Effective potential for a fixed parameter $\lambda$

The parameter  $\lambda$ , which determines the stability of the system is a function of variables describing the controlled object (this variable is the length of the pendulum) and variables controlling the pendulum ( $A, \Omega$ ). Equations (20), (21), (22) show that for any angle  $\Phi$  within the range  $< 0, \pi$ ) the stability condition can be written:  $\lambda > 2$ .

This condition is satisfied for the example values:  $l = 1m$ ,  $g = 9,81 m/s^2$ ,  $A = 0,1 m$ ,  $\Omega = 70 rad/s$ , for which the parameter  $\lambda = 3,74618$ . The above-mentioned values and the pendulum mass  $m = 0,1 kg$  will be used in further analysis of the system.

Fig. 4 shows a graph of the pendulum effective potential energy as a function of the angle of oscillations the suspension point  $\beta$  and the angle  $\Phi$  with the rest system parameters set above.

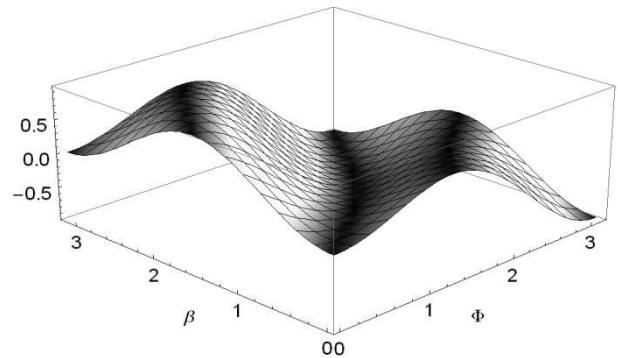


Fig. 4. Effective potential of the pendulum in function  $\beta$  and  $\Phi$

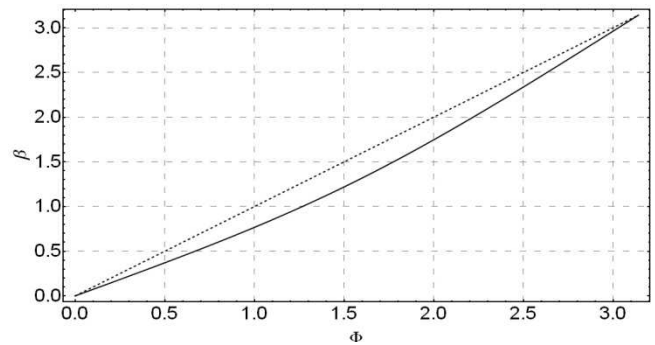


Fig. 5. The relationship between  $\beta$  and  $\Phi$ , at which the pendulum is at a minimum of potential

The plot's colors reflect the absolute value of the first derivative of  $U_{ef}$  – the darker the color, the lower the value of the derivative. With these colors function extremes are

more visible. The longest dark bar at the graph represents the area where the potential has a minimum value. Drawing a relationship (18) one can show this curve as in Fig. 5.

The dashed line in Fig. 5 describes the relationship  $\beta = \Phi$ . The function (18) shows that with increasing  $\lambda$ , the function more and more „closes" to the relationship  $\beta = \Phi$ . This behavior becomes evident after analysis of the formula (14) describing the  $U_{ef}$ . The first term of this formula comes from the gravitational potential and the other from the oscillations. With increasing  $\lambda$  the second term begins to dominate over the gravity and takes the highest absolute value (for fixed  $\lambda$ ), when  $\beta = \Phi$ .

**5. NUMERICAL SIMULATION RESULTS**

If the parameter  $\lambda$  does not change in the experiment (and of course satisfies the stability conditions), the only problem to solve is to determine the angle at which we want to set the pendulum and then, according to (18), determine the angle  $\beta_{ext}$  which will determine the direction of vibration of the pendulum suspension point. This chapter will be presenting numerical results for the specific values of the angle  $\Phi$ . The parameters of the system ( $g, m, l, A, \Omega$ ) are the same as those listed in Section 4.1, the parameter  $\lambda = 3,74618$ . The simulation is the numerical solution of equation (7).

**5.1. Example 1:  $\Phi = \pi/4$**

The direction of oscillations according to (18):  $\beta = 0,5918$ .

Initial conditions:  $\theta(0) = \pi/4 + 0,1 \text{ rad}$ ,  $\dot{\theta}(0) = 0 \text{ rad/s}$ .

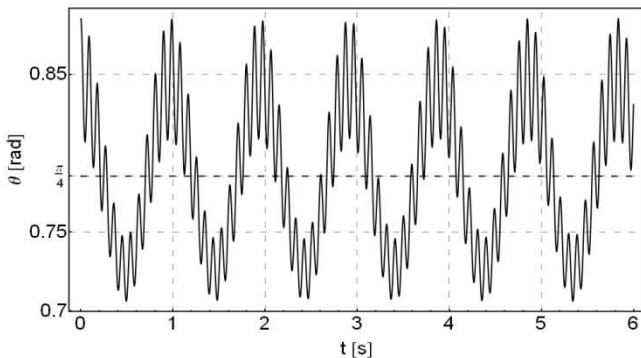


**Fig. 6.** Numerical simulation result of equation (7)

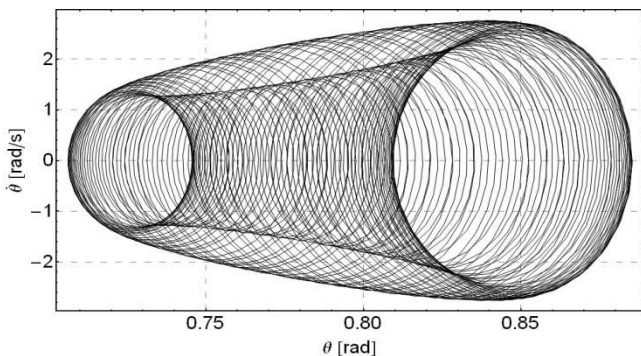


**Fig. 7.** Phase portrait of the simulation

Figs. 6 and 7 show the simulation results of the pendulum motion. As you can see the pendulum inclined to a certain angle starts to oscillate around the set point, in this case equal to  $\pi/4$ . Effective potential for this case has the form as shown:

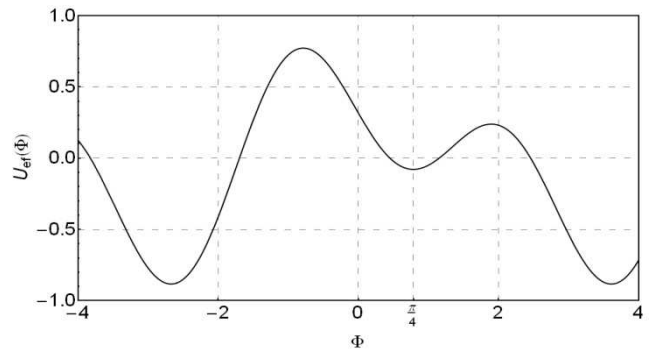


**Fig. 8.** Effective potential of the pendulum

As shown in Fig.8, the potential has a minimum for the desired angle.

**5.2. Example 2:  $\Phi = \pi/2$**

The direction of oscillations according to (18):  $\beta = 1,289$ .

Initial conditions:  $\theta(0) = \pi/2 + 0,1 \text{ rad}$ ,  $\dot{\theta}(0) = 0 \text{ rad/s}$ .

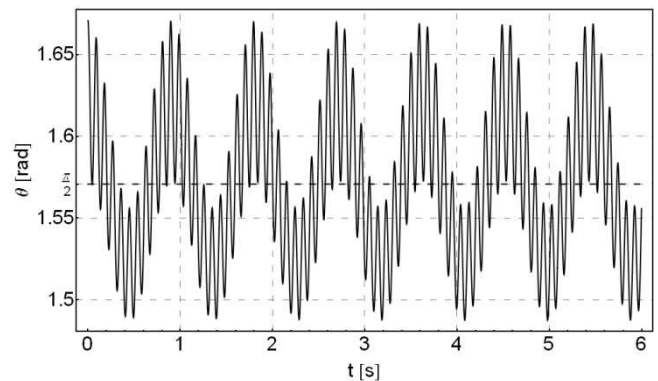


**Fig. 9.** Numerical simulation result of equation (7)

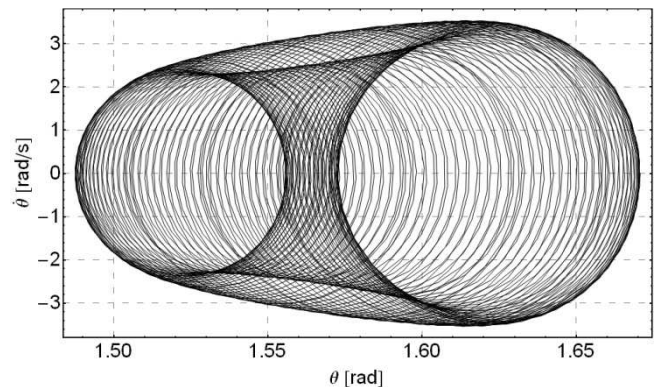


**Fig. 10.** Phase portrait of the simulation

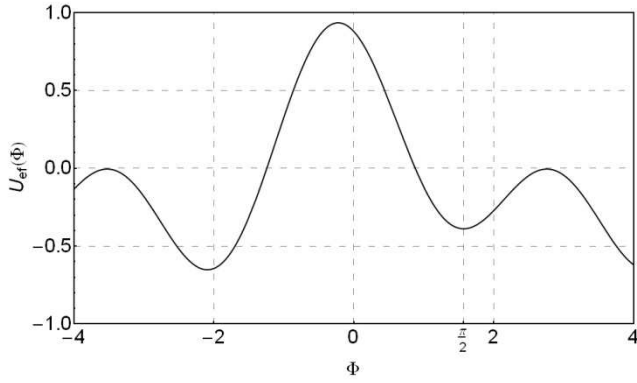


**Fig. 11.** Effective potential of the pendulum

These figures illustrate the results of the numerical simulation of the pendulum for  $\Phi = \pi/2$ . As you can see the system behaves as planned. In Fig. 9, and even better on the phase portrait can be seen increase of the speed of fast oscillations relative to the first example. The frequency of fast oscillations seems to be the same in both examples.

### 5.3. Example 3: $\Phi = 3/4\pi$

$\beta = 2,162, \theta(0) = 3/4\pi + 0,1 \text{ rad}, \dot{\theta}(0) = 0 \text{ rad/s}$ .  
 The following figures show the simulation results.

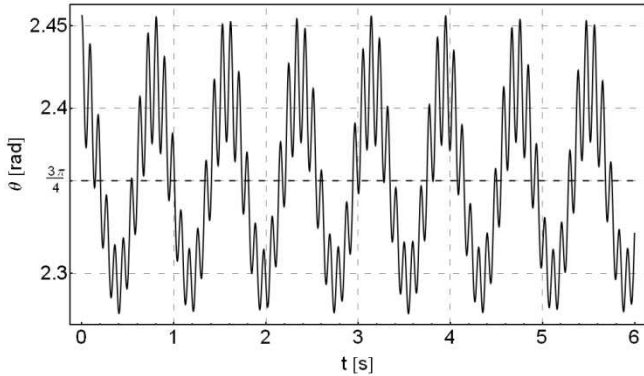


**Fig. 12.** Numerical simulation result of equation (7)

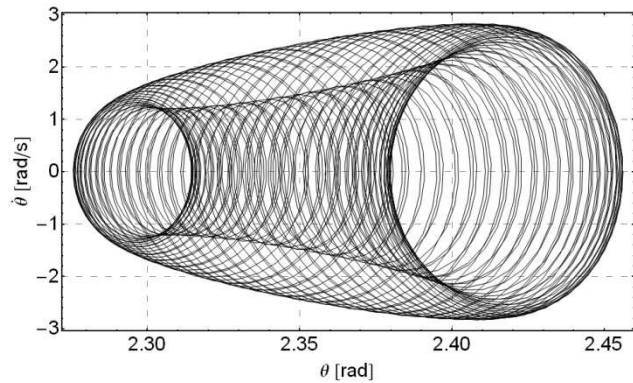


**Fig. 13.** Phase portrait of the simulation

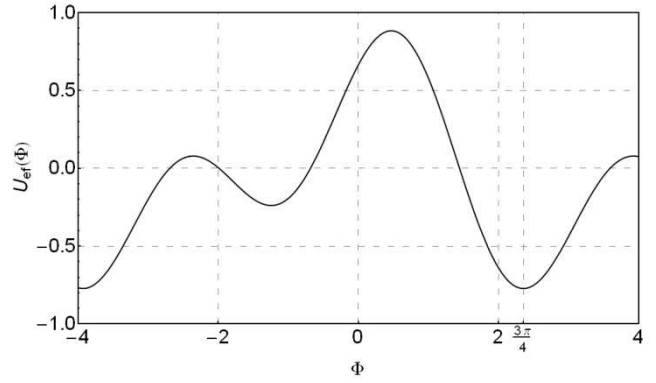


**Fig. 14.** Effective potential of the pendulum

The figures above illustrate the results of numerical simulation of the pendulum for  $\Phi = 3/4\pi$ .

## 6. NUMERICAL SIMULATION IN THE PRESENCE OF FRICTION FORCE AND RANDOM DISTURBANCES

The results presented in chapter five, illustrate behavior of the perfect system, that is, without energy dissipation and noise. In the real world, forces of friction and random disorders cannot be eliminated. To make the system more realistic, numerical simulation in presence of non-conservative forces was performed.

The Euler-Lagrange equation then takes the form:

$$\frac{d}{dt} \frac{\partial L}{\partial \dot{\theta}} - \frac{\partial L}{\partial \theta} = -k_1 \dot{\theta} + k_2 \varepsilon(t) \quad (23)$$

where:  $k_1$  – viscous damping coefficient,  $k_2$  – noise coefficient.

$\varepsilon(t)$  is a random disturbance and is assumed to obey normal distribution with density function:  $\frac{1}{\sqrt{2\pi}} e^{-\frac{\varepsilon(t)^2}{2}}$ .

The average value of  $\varepsilon(t)$  is zero. The perturbation changes randomly at each simulation time step. Fig. 15 illustrates an example of the function  $\varepsilon(t)$ .

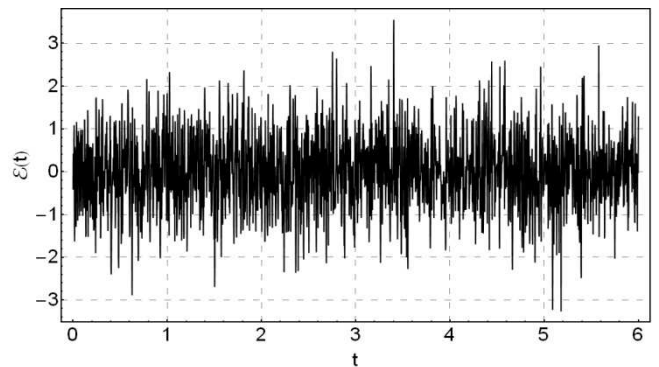


**Fig. 15.** Random perturbations of the system

Solution of the equation (23) gives the result:

$$\ddot{\theta} = \frac{3(A\Omega^2 \sin(\beta - \theta) \cos(t\Omega) + g \sin(\theta))}{2l} - \frac{3k_1}{l^2 m} \dot{\theta} + \frac{3k_2}{l^2 m} \varepsilon(t) \quad (24)$$

The obtained equation is an equation of the pendulum's motion in the presence of friction force and random disturbances.

While the viscous friction should help to maintain the pendulum in the desired position, a random disturbance can cause loss of the system's stability. This will happen when the pendulum "jumps out" from an effective potential well on the result of existing disturbances. So the critical value of the parameter  $k_2$  depends on the depth of potential well. The parameter  $k_2 = 0,03Nm$  will be used in further analysis of the system. For such value of the coefficient  $k_2$ , some distortions have been noticed, but the system has still been stable. The adopted value of the damping factor is:  $k_1 = 0,02Nm$ . The initial conditions and the angle  $\beta$  values are the same as in the examples in chapter 5.

**6.1. Example 1:  $\Phi = \pi/4$**

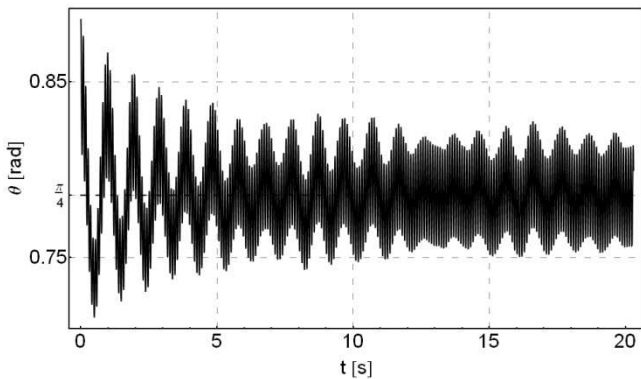


**Fig. 16.** Numerical simulation result of equation (24)

As shown in Fig. 16, high-amplitude oscillations are damped. Small amplitude and high frequency vibrations still occur. The presence of small oscillations is the result of the suspension point's vibrations. Force caused by these vibrations is so large that the friction is not able to dampen the pendulum. You can verify if the random disturbance force cause these small oscillations. Fig. 17 shows the result of the simulation, for the parameter  $k_2 = 0Nm$ .

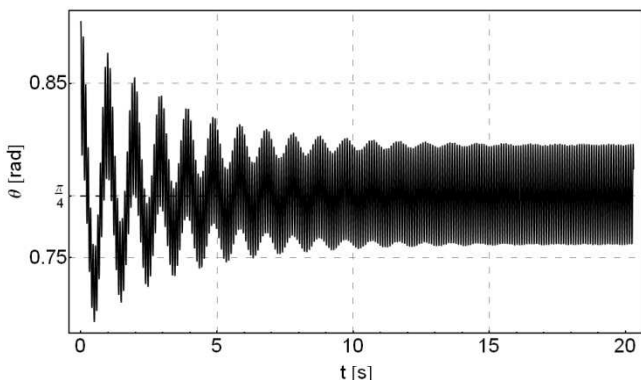


**Fig. 17.** Numerical simulation result of equation (24) for  $k_2 = 0$

As shown in Fig. 17 the system still performs small vibrations. The simulations show that the random force introduces only a small disturbance to vibration.

To demonstrate the resistance of the system to disturbances, additional simulations were performed for the parameter  $k_2 = 0,3Nm$  and  $k_2 = 1,7Nm$ . The results of these simulations are illustrated in Figs. 19 and 20.

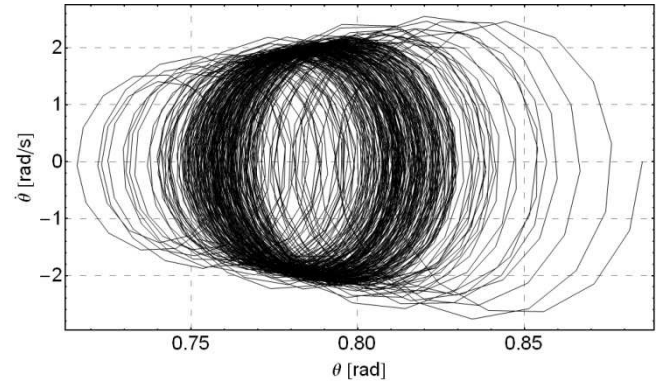


**Fig. 18.** Phase portrait of the simulation with random noise

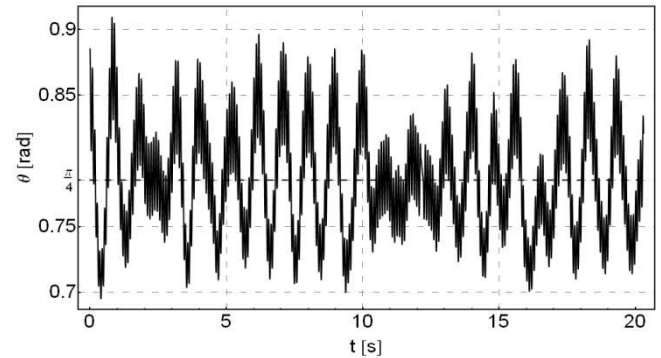


**Fig. 19.** Numerical simulation result of equation (24) for  $k_2 = 0,3Nm$

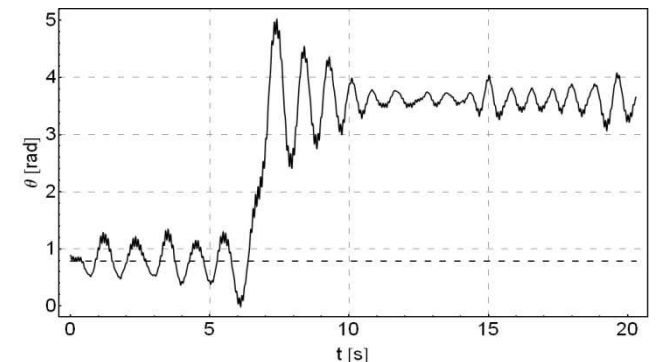


**Fig. 20.** Numerical simulation result of equation (24) for  $k_2 = 1,7Nm$

Fig.19 shows that 10-times greater disturbance does not cause loss of stability. For  $k_2 = 1,7Nm$  (Fig. 20) system is no longer stable and the pendulum "jumps" to the neighboring potential well (see Fig. 8).

**6.2. Example 2:  $\Phi = \pi/2$**

As in the first example, the system performs small, rapid oscillations around the set point. Just as in the case without friction and disturbances, the speed of pendulum oscillations is greater than in example  $\Phi = \pi/4$ .

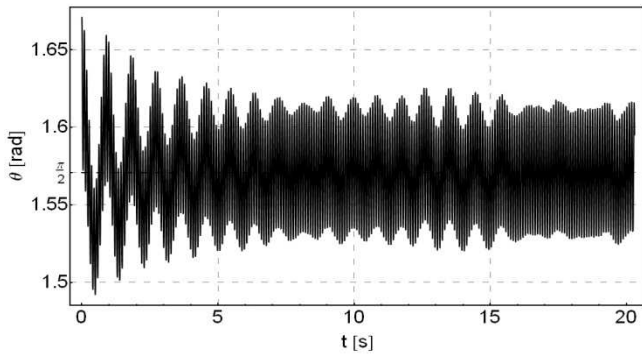


Fig. 21. Numerical simulation result of equation (24)

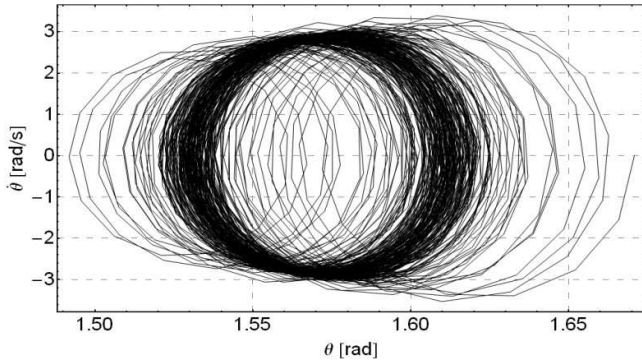


Fig. 22. Phase portrait of the simulation

### 6.3. Example 3: $\Phi = 3/4\pi$

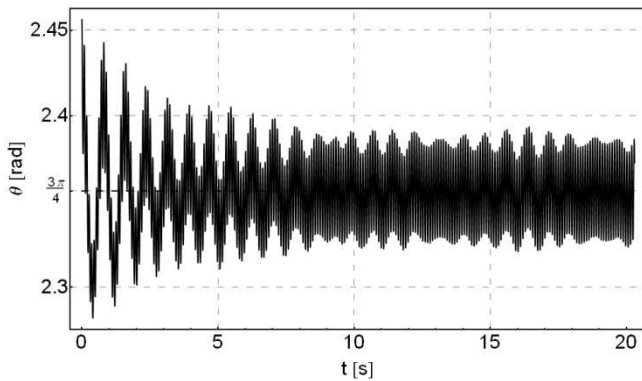


Fig. 23. Numerical simulation result of equation (24)

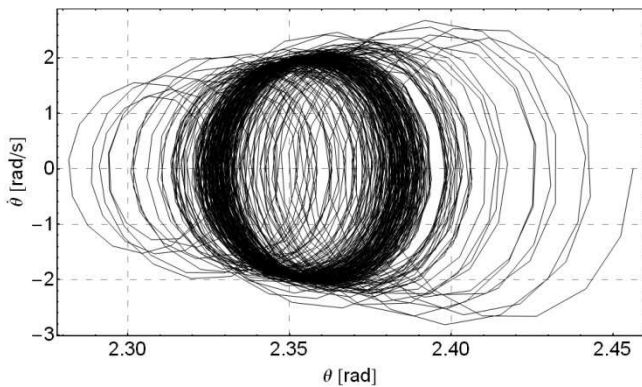


Fig. 24. Phase portrait of the simulation

The figures above illustrate the results of numerical simulation of the pendulum for  $\Phi = 3/4\pi$ .

## 7. SUMMARY

The results presented in this paper demonstrate the possibility of stabilizing the pendulum in various inclinations. The system is stable if its parameters satisfy the conditions that have been set in chapter four. In addition to solutions for the "ideal" system, the possibility of stabilizing the pendulum in the presence of friction force and random disturbances has been demonstrated. It is shown that the system is highly resistant to disturbances, which increases the chances of an experimental realization of the system.

## REFERENCES

1. **Astrom K. J, Murray R. M.** (2008), *Feedback Systems: An Introduction for Scientists and Engineers*, Princeton Univ Pr.
2. **Kapitza P. L.** (1951), *Majтник s vibrirujuwim podvesom*, Uspekhi Fizicheskikh Nauk.
3. **Landau L. D., Lifszyc J.M.** (2007), *Mechanika*, PWN, Warszawa.
4. **Siemieniako F., Ciężkowski M.** (2011), Sterowanie położeniem odwróconego wahadła w pętli otwartej, Wojciech Tarnowski, Tomasz Kiczowski (red.): *Poliptymalizacja i Komputerowe Wspomaganie Projektowania*, Mielno 2011, Wydawnictwo Uczelniane Politechniki Koszalińskiej, Koszalin 2011, str. 31-39.